

Abubakar Hamisu\* and Sevim Ü. Çelik

# Poly(AN-co-PEGMA)/hBN/NaClO<sub>4</sub> composite electrolytes for sodium ion battery

<https://doi.org/10.1515/epoly-2017-0022>

Received January 22, 2017; accepted July 4, 2017; previously published online August 12, 2017

**Abstract:** Polymer electrolytes composed of an acrylonitrile and polyethylene glycol methacrylate copolymer poly(AN-co-PEGMA) with addition of NaClO<sub>4</sub> are studied by impedance spectroscopy, differential scanning calorimetry (DSC), fourier transform infrared (FTIR), X-ray diffraction (XRD), scanning electron microscopy (SEM) and thermogravimetric analysis (TGA). Hexagonal boron nitride (hBN) particles are having increasing interest owing to mechanical properties, thermal stability, chemical stability and good lubrication property. In this study, hBN was used as an inorganic filler. FTIR spectroscopy was used to examine the interactions between the host polymer and both NaClO<sub>4</sub> salt and nano hBN particles. The thermal properties of the composites were studied using TGA and DSC tests. TGA results showed that all the composites membranes were thermally stable till 300°C with one step degradation. Surface morphology of the films was examined with SEM which also reveals the homogeneous dispersion of nano hBN in the polymer matrix. Ionic conductivity was studied with impedance spectroscopy, the results showed that the ionic conductivity increases with increasing PEGMA ratio. ANcoPEGMA 11 20Na (EO:Na ratio=20) sample showed maximum ion conductivity of approximately  $3.6 \times 10^{-4}$  S cm<sup>-1</sup> at 100°C. This is because ANcoPEGMA 11 20Na has highest percentage of PEGMA and highest number of Na<sup>+</sup> ion per EO groups.

**Keywords:** copolymer; hexagonal boron nitride; NaClO<sub>4</sub>; Na-ion conductivity; polymer nanocomposite; sodium ion battery.

## 1 Introduction

Lithium ion batteries (LIBs), the most popular type of secondary batteries are used in almost all portable electronic

devices, are a feasible solution to the larger world energy consumption concerns (1). Electrochemistry of lithium based cell provides various attractive attributes: lithium is the lightest metal with an exceptional low redox potential ( $E_{\text{Li}^+/\text{Li}} = -3.04$  V versus standard hydrogen electrode). Moreover, lithium ion possesses a small ionic radius which is advantageous for easy diffusion into solid. They also have a long cycle life with high rate capability which also depends on electrodes employed and species that de/intercalates between them. These properties made Li-ion technology confined to the market of portable electronics (2). Unfortunately, the lithium element has limited resources. The relative abundance of lithium in the Earth's crust is only 20 ppm (3, 4). Thus, many researchers commit themselves to explore new abundant and low-cost alternatives to LIBs in the Earth such as sodium-ion batteries (SIBs) (2, 4, 5) and calcium-ion batteries (CIBs) (6, 7). Sodium is available in a high abundance with a low cost: natural sodium is more than 1000 times more abundant than lithium. It can be obtained from both deposits in the Earth's crust and salt water (4). Sodium has very desirable redox potential ( $E_{\text{Na}^+/\text{Na}} = -2.71$  V versus standard hydrogen electrode: only 0.3 V greater than that of lithium) and also has electrochemical similarities with lithium which have been intensively explored. By following the terminology of LIBs and these desirable properties of sodium, SIBs can be the ideal alternative to LIBs.

Faster development of SIBs can be attributed to the analogous behaviors already known from the studies of the LIBs. SIBs comprise anode electrode, cathode electrode, electrolyte, and porous separator in case of liquid electrolyte. Layered oxide with tertiary or greater transition metals have demonstrated to give the greatest performance among reported cathode materials (4). Promising anodes are sodium alloying metals composites and carbon. SIB and LIB has the same working principle (4). In the case of liquid electrolyte, the electrolyte for both is a mixture of organic solvents with dissolved metal salt (~1 M). However, the issues encountered within LIBs also happen within the SIBs including using liquid electrolytes where electrolyte leakage may occur and other safety-related concerns (8). Due to these concerns, solid polymer electrolytes (SPE) are an appealing alternative to replace liquid electrolyte systems.

Electrolytes of all electrochemical energy storage such as batteries are classically given less attention as

\*Corresponding author: Abubakar Hamisu, Department of Chemistry, Kano University of Science and Technology Wudil-Kano, Kano, Nigeria, Tel.: +2348039352016, Fax: +2348039352016, e-mail: ababakary@gmail.com

Sevim Ü. Çelik: Department of Chemistry, Fatih University, 34500 B.Çekmece-İstanbul, Turkey

compared to the active materials (the electrodes) (5, 9). The reason behind this is because that the electrodes properties define the system energy density (volumetric and gravimetric) and hence are most eye-catching. But the role of the electrolyte should, nevertheless, not be disregarded because it is importantly responsible for life-length and realistic possible performance in terms of practical reachable rate capability, safety, capacity, etc. These impressions are now being actualized by the broader part of battery research and development (R&D) (9). Also, together with the development of novel techniques analysis, disclosing the task of the electrolytes in gaining the best promising interfaces to the electrodes and hence full performance of the cell (9). In fact, the electrolyte which ionically links the electrodes is one of the essential aspects that inspire the performance of battery. Utmost research on battery makes use of liquid electrolytes. Researchers usually use the metal salts (Li, Na, Mg, etc) in different non-aqueous organic solvents as the liquid electrolytes (5). Conventional batteries mostly comprise of liquid electrolyte, that aids Li ions transport back and forth between the anode and cathode (10). This leads to the high probability of electrolyte leakage if in any case holes are present; this is one of the foremost conventional batteries disadvantages. Dendrites ion formation is another dilemma of the liquid electrolyte battery, which make an increasing chance of explosion (10). To overcome these problems, solid electrolyte can be placed in between the cathode and the anode of the battery. This is the fundamental principle idea underlying the solid state battery (10). As compared to liquid electrolytes, SPEs possess several advantages such as promising mechanical properties, easy fabrication into thin films of desirable size, and the ability to form efficient electrode-electrolyte contacts (11, 12). An early work on polymer electrolyte was carried out in the 1970s, when Fenton et al. (13) showed that a nonconducting polymer, polyethylene oxide, started conducting when lithium salt was added into the polymer matrix. Several researches on sodium-ion polymer electrolytes have been reported, such as poly(ethylene oxide) (PEO) (14) and polyvinyl alcohol (PVA)-based polymer-salt complexes comprising NaPF<sub>6</sub>, NaClO<sub>4</sub>, NaTFSI, NaFSI, NaTf, Na<sub>2</sub>SO<sub>4</sub>, NaCF<sub>3</sub>SO<sub>3</sub> and NaPO<sub>3</sub> sodium salts (15–18). The most extensively studied polymer host for solid polymer electrolyte applications is PEO. This is due to its high electrochemical stability in comparison with other polyethers, copolymers or PEO-branched polymers (8). SPEs for SIBs simply comprise a sodium salt dissolved in a polymer matrix, the latter usually being poly(ethylene oxide) because of its effectiveness in dissolving alkali metal salts (13). For polyether based electrolytes, ions transport is supported by segmental motion of polymer chains. Thus, conductivity of such systems decreases on cooling to glass

transition temperature or during crystallization, which immobilizes segments of the chain (19). Preserving amorphous state of salt can be achieved by interactions between salt and polymer matrix. Among different polymers, polyacrylonitrile PAN has been found to be promising for that application. Ferry et al. (20) has shown that PAN is involved in dissolution of the salt and thus suppression of the salt precipitation process. Following the trend of sodium battery research, studies on sodium SPEs were performed since the 1990s and has regained attention quite recently (21). To date, different combinations of Na-salts and PEO have been considered, mostly mimicking the much more researched lithium based SPEs.

Composite polymer electrolytes have received increasing interest for the past two decades because of their exciting bulk and surface properties (22). Controlling polymers nanostructure by the addition of nano particles had supported the structural and functional property improvements in various systems of polymer as a material answer to incessant demands for advanced industrial sectors (23). The accessibility of new nano particles having astonishing properties has led to exciting possibilities in continuous extension of markets of the polymers (23). Ionic conductivities of sodium and lithium PEO-based SPEs are very comparable and both rather modest;  $10^{-5}$ – $10^{-6}$  S cm<sup>-1</sup> at room temperature (21). Fuentes et al. (24) demonstrated Na<sup>+</sup> ions can provide higher conductivity, or at least a comparable conductivity to that of Li<sup>+</sup> ions in the same basic material. This provides an excellent possibility to use Na<sup>+</sup> ions as a new generation of batteries, instead of lithium. Li<sup>+</sup> and Na<sup>+</sup> salts showed opposite dc-conductivity behavior with two anions. At 40°C, the conductivity values change from  $1.05 \times 10^{-2}$  S cm<sup>-1</sup> (Li[COSANE]) and  $1.75 \times 10^{-2}$  S cm<sup>-1</sup> (Na[COSANE]) to  $2.8 \times 10^{-3}$  S cm<sup>-1</sup> (Li[TPB]) and  $1.5 \times 10^{-3}$  S cm<sup>-1</sup> (Na[TPB]) (24). Hexagonal boron nitride (hBN) is basically an important material with combination of unique properties. It has been used in matrix for ceramic composites to decrease thermal expansion coefficient, improving thermal shock resistance of the composite and enhancing machinability (25). Moreover, hBN has also been used in matrix for polymer composites to enhance flame retardant and toughness properties (26).

In this work a copolymer of acrylonitrile and polyethylene glycol methacrylate (PEGMA) was synthesized, poly(AN-co-PEGMA). The poly(AN-co-PEGMA) was used as matrix to prepare composite polymer electrolytes with different mole ratio of NaClO<sub>4</sub> and nano-hBN as a filler. The effect mole ratio of NaClO<sub>4</sub> salt was investigated to see how it affects both conductivity and thermal properties of the polymer electrolytes. Nano-hBN was employed in order to improve thermal property of the polymer

electrolytes. The polymer electrolytes were characterized using FT-IR, X-ray diffraction (XRD), thermogravimetric analysis (TGA), differential scanning calorimetry (DSC) and scanning electron microscopy (SEM) analysis. Na-ion conducting properties of the materials were studied by dielectric-impedance and the results were discussed and compared with previous reported studies.

## 2 Experimental

### 2.1 Materials

Sodium perchlorate (NaClO<sub>4</sub>) (≥98.0%), polyethylene glycol methacrylate (PEGMA, M<sub>n</sub> = 360 g mol<sup>-1</sup>), ethyl ether and acetonitrile (≥99.9%) were purchased from Sigma-Aldrich. Dimethylformamide (DMF), azobisisobutyronitrile (AIBN) and acrylonitrile (AN) were purchased from Merck. Hexagonal boron nitride (hBN) (99% Pure, APS: 70 nm) was purchased from lowerfriction, Canada.

### 2.2 Preparation of the samples

A copolymer of acrylonitrile (AN) and poly glycol methacrylate (PEGMA) with an average molar mass of AN m.u. (monomeric unit) to PEGMA m.u. equal to 1:1, 1:0.5 and 1:0.25 were synthesized by dissolving required amount of AN and PEGMA in 30 ml of DMF and stirred for 15 min in a reaction flask. One percent of AIBN initiator was added into the reaction flask to initiate copolymerization reaction. The reaction was allowed for 5 h and it is shown in Figure 1. The copolymers were then washed with ethyl ether to remove unreacted monomers and initiator. The copolymers were blended with NaClO<sub>4</sub> salt (EO:Na=0, 20 and 30) and 5% hBN (w/w) in 10 ml of acetonitrile to form a solution. The solution was stirred till homogeneous mixture was obtained. The composites were prepared by casting the solution on Teflon dish and dried in two stages. In the first stage solvent had been removed by evaporation

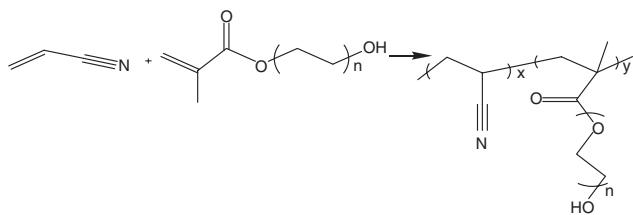


Figure 1: Copolymerization reaction.

under normal environmental condition. In the second stage, the samples were placed under vacuum 200 mm Hg at 60°C for 48 h in order to remove all traces of solvent followed by conditioning in an Ar-filled glove box for 24 h.

### 2.3 Characterization

FTIR spectrometer Bruker alpha-P equipped with an ATR module was used to register the spectra in the range of 4000–400 cm<sup>-1</sup> in order to observe the functional groups and their interaction in the system.

The polymer electrolytes thermal stabilities were analyzed with Perkin Elmer STA 6000 Thermal Analyzer. The samples were heated from 30°C to 750°C under N<sub>2</sub> atmosphere at a scanning rate of 10°C min<sup>-1</sup>.

PerkinElmer JADE differential scanning calorimetry (DSC) was used to investigate the thermal transitions of the samples. The samples (~10 mg) were put into aluminum pans. In heat flux instruments, the sample and reference are heated from the same source and the amount of heat necessary to keep the reference and the sample at the same temperature were measured. During the measurements, firstly, the samples were heated from 0 to 150°C, and then, they were cooled from 150 to 0°C. Finally, the second heating was performed from 0 to 250°C at a rate of 10°C min<sup>-1</sup> under nitrogen atmosphere.

Surface morphology of the samples was examined by SEM, JEOL-7001 FESEM (Tokyo, Japan). Prior to the SEM measurements all of the samples were coated with gold for 150 s in a sputtering device.

XRD patterns of the polymer electrolytes and pure hBN were obtained by XRD instrument, Rigaku Smart Lab Diffractometer operated at 40 kV and 35 mA using Cu-K $\alpha$  radiation having wavelength ( $\lambda$ ) of 1.54059 Å. The XRD peaks were recorded in the 2 $\theta$  range of 10°–70°.

Ionic conductivity measurements were carried out using a Novocontrol dielectric-impedance analyzer. The membranes were sandwiched between platinum blocking electrodes, and the conductivities were measured in frequency range 1 Hz and 3 MHz at 10°C intervals. The temperature was controlled with a Novocontrol cryosystem.

## 3 Results and discussion

A copolymer of acrylonitrile and polyethylene glycol methacrylate (PEGMA) was synthesized. The PEGMA was used to reduce the hardness of poly acrylonitrile for good conductivity result. Composite electrolytes, poly(AN-co-PEGMA)/hBN/NaClO<sub>4</sub> (ANcoPEGMA-xNa) were prepared

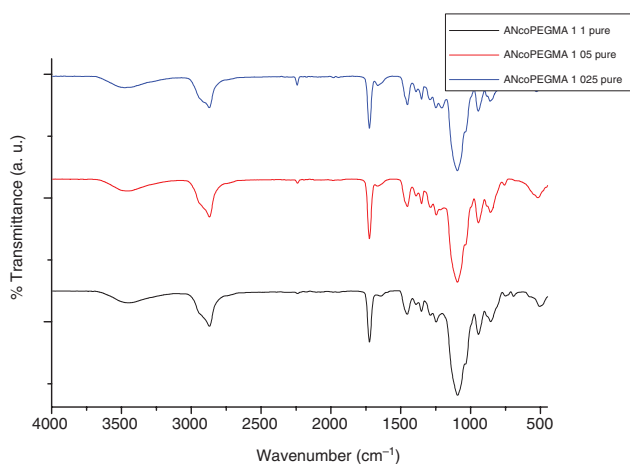


Figure 2: FTIR result of the pure poly(AN-co-PEGMA) copolymer.

with different mole ratio of NaClO<sub>4</sub> and PEGMA ratio. The interaction between the host polymer and the ions were studied with FTIR.

### 3.1 FTIR study

FTIR analysis was conducted in order to verify the formation of the copolymer of AN and PEGMA. And also to investigate the interactions between NaClO<sub>4</sub> salt and the copolymer host, and incorporation of hBN nanoparticle into poly(AN-co-PEGMA). The FT-IR results of three pure poly(AN-co-PEGMA) copolymers with different AN:PEGMA ratio (1:1, 1:0.5 and 1:0.25) were compared in Figure 2. The distinctive stretching vibrations appearing at 2239 cm<sup>-1</sup> is attributed to C≡N nitrile group of the copolymer (27, 28). The band at 2877 cm<sup>-1</sup> is attributed to stretching vibrations of the aliphatic C-H groups. Bands at 1452 cm<sup>-1</sup> and 1347 cm<sup>-1</sup> are attributed to symmetrical and asymmetrical bending vibration C-H groups in CH and CH<sub>2</sub> (27). The peaks at 1728 cm<sup>-1</sup> and 1091 cm<sup>-1</sup> represent C=O and C-O stretching vibrations for carbonyl group of carboxylic ester. The wide band at 3441 cm<sup>-1</sup> represents the O-H stretching vibration. The band at 952 cm<sup>-1</sup> from the monomers peaks (AN and PEGMA) Figure 3 which is attributed to C=C disappeared, this is due to the disappearing of C=C double bond during copolymerization reaction.

AN:PEGMA ratios were confirmed since the copolymerization % yield is approximately 100%. Furthermore, the ratios were roughly estimated by comparing the peak intensity of the copolymers with different ratio (1:1, 1:0.5 and 1:0.25). Intensity of the peak at 2239 cm<sup>-1</sup> (ν C≡N) increased as the PEGMA ratio decreased from 1 to 0.25 (Figure 2) i.e. the percentage of acrylonitrile group of

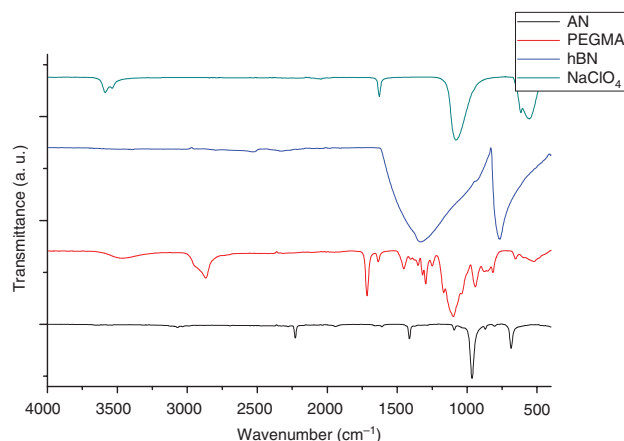


Figure 3: FTIR result of AN, PEGMA, hBN and NaClO<sub>4</sub>.

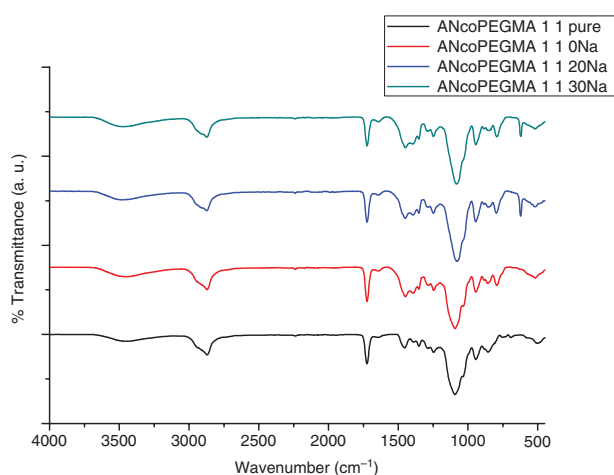
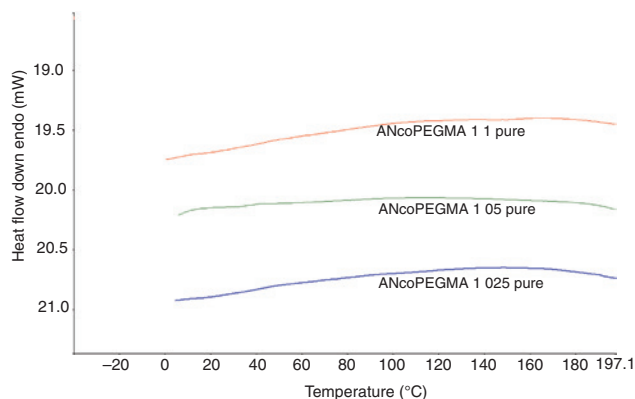


Figure 4: FT-IR results of pure poly(AN-co-PEGMA) (AN:PEGMA 1:1) and ANcoPEGMA 11 xNa composite electrolytes (x; EO:Na = 0, 20 and 30).

poly(AN-co-PEGMA) increased. Also the intensity of the peak at 1091 cm<sup>-1</sup> (ν C-O) decreased as the PEGMA ratio decreased from 1 to 0.25 Figure 2, i.e. the percentage of PEGMA group decreased. Figure 4 represent FT-IR results of pure poly(AN-co-PEGMA) (AN:PEGMA 1:1) and 5% hBN, ANcoPEGMA 11 xNa composite electrolytes (x=0, 20 and 30, i.e. EO:Na ratio = 0, 20 and 30). There is broadening around 1336 cm<sup>-1</sup> to 1481 cm<sup>-1</sup>, which is due to the incorporation of hBN nanoparticle. Peak at 622 cm<sup>-1</sup> Figure 4 is attributed to ClO<sub>4</sub><sup>-</sup> group of NaClO<sub>4</sub> (8).

### 3.2 DSC analysis

From the literature pristine PAN homopolymer was recorded to have T<sub>g</sub> around 95°C (29) and PPEGMA around -57°C (30). In studying the thermal behavior of the copolymer, DSC scanned from -50°C to 250°C. The DSC results of



**Figure 5:** DSC curves of pure poly(AN-co-PEGMA) copolymers at a heating rate of 10°C min<sup>-1</sup>.

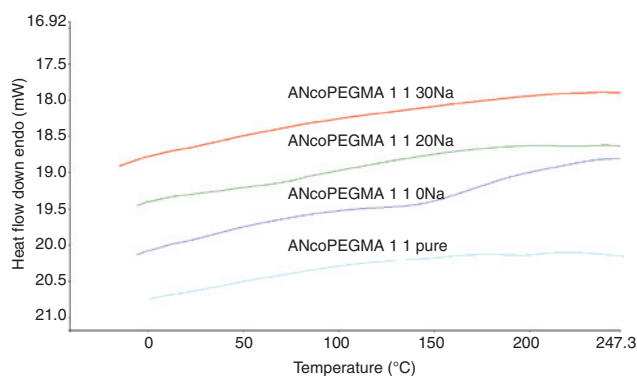


**Figure 6:** DSC curves of ANcoPEGMA 1 1 xNa composites ( $x$ ; EO:Na = 0, 20 and 30) at a heating rate of 10°C min<sup>-1</sup>.

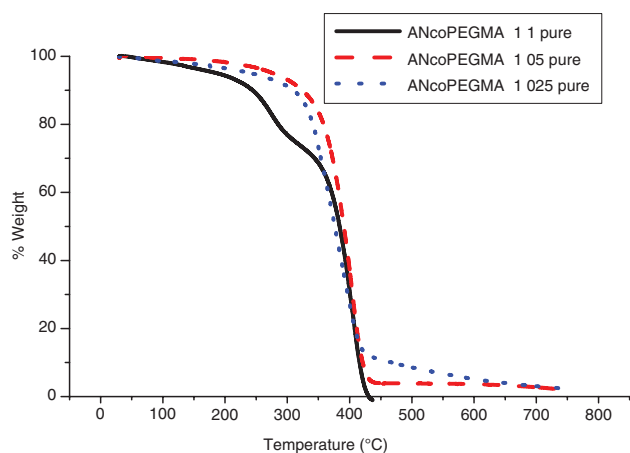


**Figure 7:** TGA result of pure poly(AN-co-PEGMA) copolymers.

the three pure copolymers (AN:PEGMA ratio; 1:1, 1:0.5 and 1:0.25) and the ANcoPEGMA 1 1 xNa composite electrolytes ( $x$ ; EO:Na = 0, 20 and 30) were depicted in Figures 5 and 6, respectively. It can be seen that no glass transition

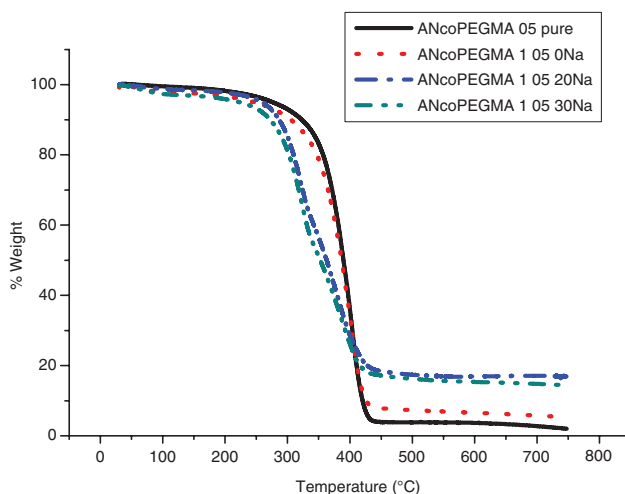


**Figure 8:** TGA results of ANcoPEGMA 1 05 xNa composites ( $x = 0, 1$  and 2).

temperature ( $T_g$ ), melting point ( $T_m$ ), or crystallization temperature ( $T_c$ ) was observed.

### 3.3 TGA

Thermal stability is one of the most important properties for polymer electrolytes (PEs) in the application of SIBs. TGA gives information about the possible physical and chemical changes that may happen during a thermal excitation in a polymer electrolyte (PE) when it is applied to working systems (31). Pure PAN and PPEGMA homopolymers are reported to have decomposition temperatures at around 340°C (32) and 250°C, respectively.

Prior to the measurement, the pure copolymer and the composites were dried under vacuum at 45°C for 24 h. Figure 7 illustrates TGA results of the neat copolymers. It can be seen that pure ANcoPEGMA 1 05 and ANcoPEGMA 1 025 are stable up to around 330°C and show one step degradation above that temperature. Pure ANcoPEGMA 1 1 showed two step degradation at 270°C and 330°C due to the decomposition of PEGMA and AN units, respectively. Figures 8 and 9 show TGA curves of the copolymers that include both Na salt and hBN. As 5% hBN was added to pure copolymer, there is no change in the decomposition temperature but the residue ratio is higher as expected. The addition of Na salts decreases the degradation temperature of ANcoPEGMA1-05 copolymer but it has no effect for ANcoPEGMA1 025 copolymer. The reason is ANcoPEGMA1 025 has lower Na ratio than ANcoPEGMA1 05. The thermal stability of all composite samples are above 250°C and suitable for polymer electrolyte applications.

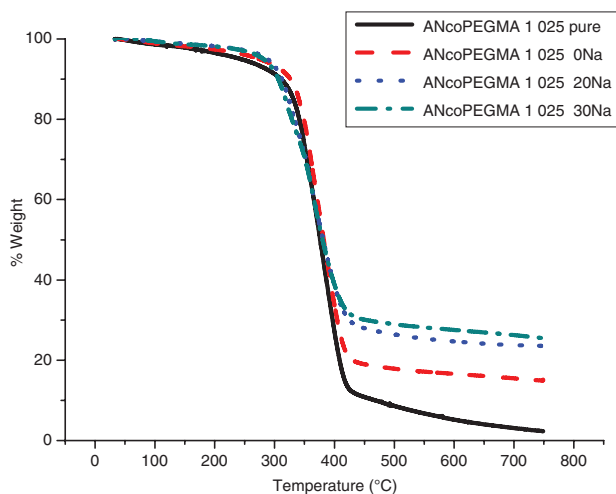


**Figure 9:** TGA result of ANcoPEGMA 1 025 xNa composite electrolytes ( $x=0, 1$  and  $2$ ).

### 3.4 SEM analysis

The SEM provides detailed photographs that give important information about the surface structure which affirms the polymer blends homogeneity (33). Several studies have reported the use of functionalized hBN which helps to

prevent agglomeration in various polymer matrices (33–35). In this study we used pure hBN without any surface modification and sonication was used just to provide homogeneity. Figure 10 shows the scanning electron micrograph (SEM) image of the composites prepared from poly(AN-co-PEGMA) copolymer via the solution casting method. As seen in the images, the composite films are homogeneous and exhibit single phase formation which indicates that hBN was uniformly distributed into the poly (AN-co-PEGMA) matrix.

### 3.5 XRD analysis

XRD analysis is a non-damaging technique which is used to analyze the existence of any phase change or crystallinity changes after blending two different materials with different crystallinity (35). Figures 11–13 show XRD patterns of pure hBN, ANcoPEGMA 11 0Na, ANcoPEGMA 11 20Na, ANcoPEGMA 1 05 0Na, ANcoPEGMA 1 05 20Na and ANcoPEGMA 1 025 0Na. From the literature neat PAN homopolymer shows a crystalline peak at  $2\theta \approx 17^\circ$  and this corresponds to orthorhombic PAN (1 1 0) reflection (27, 28, 36). This strong peak was observed in all the composites presenting the PAN part in the copolymer. For pristine hBN, four peaks were observed: at  $26.68^\circ$  for (0 0 2) plane,

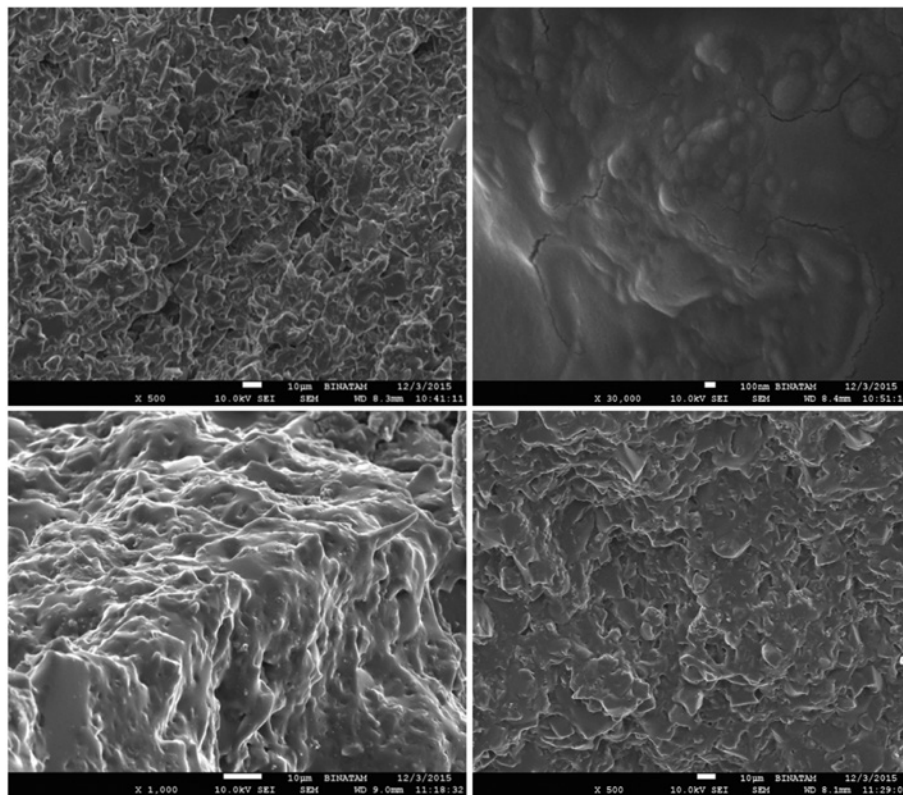


**Figure 10:** Poly(AN-co-PEGMA)/hBN/NaClO<sub>4</sub> composite electrolytes.

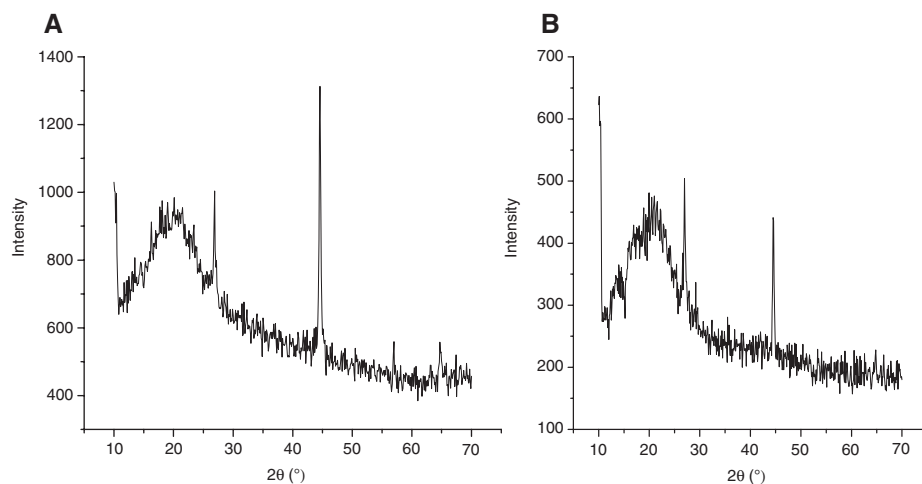


Figure 11: XRD peaks for (A) ANcoPEGMA 11 0Na and (B) ANcoPEGMA 11 20Na.

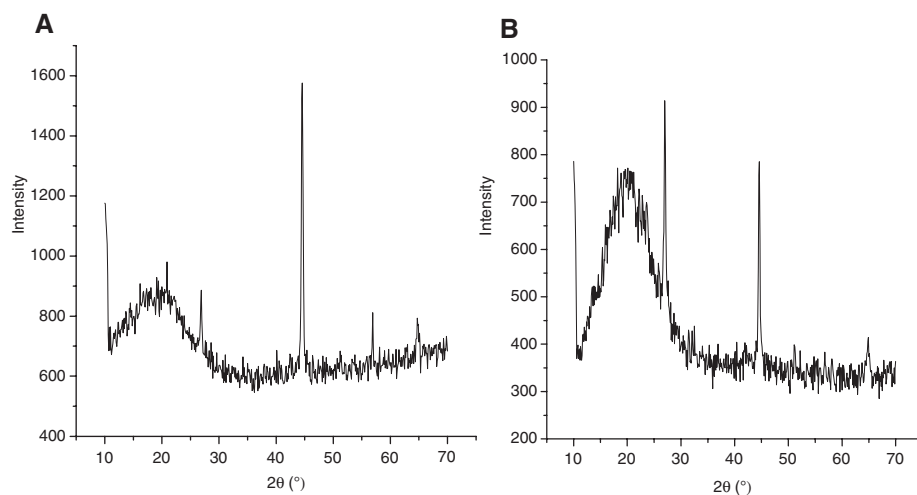


Figure 12: XRD peaks for (A) ANcoPEGMA 1 05 0Na and (B) ANcoPEGMA 11 20Na.

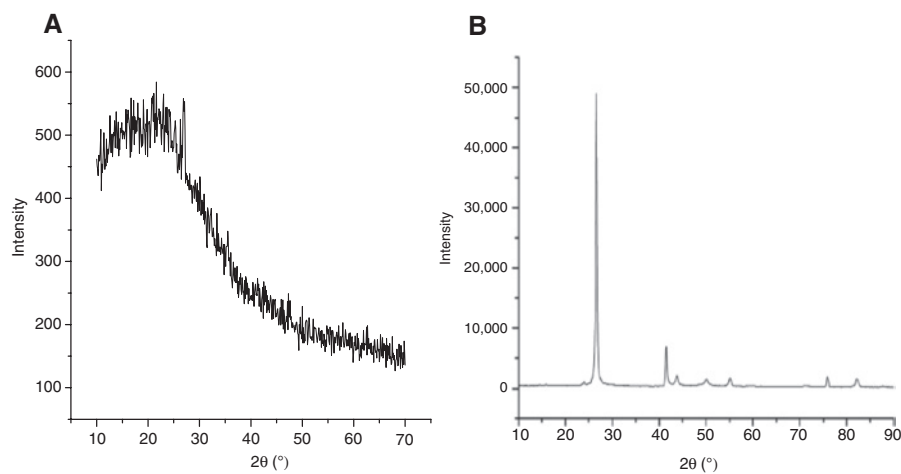


Figure 13: XRD peaks for (A) ANcoPEGMA 1 025 0Na and (B) pure hBN.

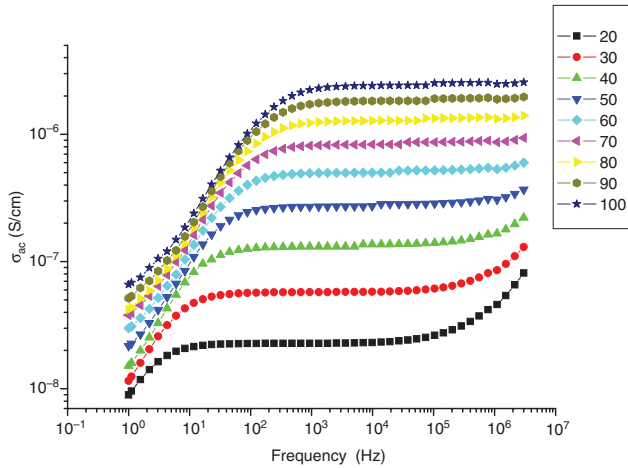


Figure 14: AC conductivity of ANcoPEGMA 11 30Na.

41.50° for (1 0 0) plane, 43.13° for (1 0 1) plane, and 55.12° for (0 0 4) planes (35).

### 3.6 Conductivity measurement

The behavior of copolymer electrolytes ionic conductivity with different AN:PEGMA ratios and different NaClO<sub>4</sub> salt %weight was studied with impedance spectroscopy. The conductivity measurement was performed in a completely water-free environment in order to avoid any contribution of humidity to the ion conductivity. The ionic conductivities of the copolymer composites were measured in the temperature range of 20°C–100°C. The frequency dependent AC conductivities,  $\sigma_{ac}(\omega)$ , of the composites were measured at various temperatures using impedance spectroscopy and equation below:

$$\sigma'(\omega) = \sigma_{ac}(\omega) = \varepsilon''(\omega)\omega\varepsilon_0 \quad [1]$$

where  $\sigma'(\omega)$  is the real part of the conductivity,  $\omega = 2\pi f$  is the angular frequency,  $\varepsilon_0$  is the vacuum permittivity ( $\varepsilon_0 = 8.852 \times 10^{-14}$  F cm<sup>-1</sup>) and ( $\varepsilon''$ ) is the imaginary part of the complex dielectric permittivity ( $\varepsilon^* = \varepsilon' - i\varepsilon''$ ) (35). The frequency and temperature dependent AC conductivities ( $\sigma_{ac}$ ) of poly(AN-co-PEGMA)/hBN/NaClO<sub>4</sub> composite electrolytes were depicted in Figure 14. There is an increase in conductivity with increasing of log frequency, which then leveled off as a result of the polarization of electrodes. The variation at the low frequency regions can be attributed to polarization, which barricades the electrode-electrolyte interface. For all composites, ionic conductivity rises with rising in temperature. This is because as temperature rises the motion of the ion becomes faster, which in turn caused an increase in ionic conduction (31).

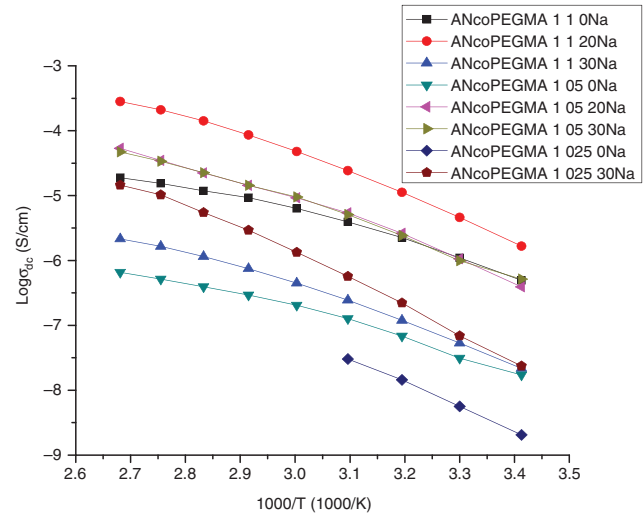


Figure 15: DC conductivity results of the composite electrolytes as a function of reciprocal temperature.

By linear fitting the plateaus of the  $\log \sigma_{ac}$  versus  $\log F$  it is possible to determine the DC conductivity ( $\sigma_{dc}$ ) of the composites. The DC conductivities of all the composites were compared in Figure 15. It is very clear from the conductivity isotherm that the DC conductivity is directly proportional to temperature. From the curve, it can also be seen that the DC conductivity also depend on AN:PEGAMA ratio and concentration of NaClO<sub>4</sub> salt. It increases as the PEGMA ratio increases. This is may be due to the softening of the copolymer, as the percentage of PEGMA content increased the copolymer became softer. As contrast to linear PEO systems, poly(AN-co-PEGMA) copolymer comprises low molecular weight PEO branches with no crystallization or melting temperature Figure 5. The conductivity also affected by EO:Na ratio. As it can be seen from Figure 15 ANcoPEGMA 11 20Na (EO:Na=20) have higher conductivity as compared with ANcoPEGMA 11 30Na (EO:Na=30). This is due to the complex formation between Na<sup>+</sup> and EO (O<sup>-</sup>) and ANcoPEGMA 11 20Na has highest number of Na<sup>+</sup> ion per EO groups.

## 4 Conclusion

Novel poly(AN-co-PEGMA)/hBN/NaClO<sub>4</sub> composite electrolytes were successfully synthesized. The successful formation of the copolymer and it's interaction with NaClO<sub>4</sub> salt was studied with FTIR. The thermal stability of all composite samples are above 250°C and suitable for polymer electrolyte applications. No T<sub>g</sub> was observed within the measured temperature. SEM images revealed the homogeneous dispersion of hBN particles. The incorporation of hBN particles into the copolymer host was also verified with XRD analysis. The ionic conductivity increases as the

PEGMA ratio and temperature increases. ANcoPEGMA 11 20Na showed maximum ion conductivity of approximately  $3.6 \times 10^{-4} \text{ S cm}^{-1}$ . With a little improvement of ionic conductivity, poly(AN-co-PEGMA)/hBN/NaClO<sub>4</sub> composite can be a good candidate for SIBs polymer electrolyte.

## References

1. Tarascon J-M, Armand M. Issues and challenges facing rechargeable lithium batteries. *Nature* 2001;414:359–67.
2. Ellis BL, Nazar LF. Sodium and sodium-ion energy storage batteries. *Curr Opin Solid State Mater Sci*. 2012;16:168–77.
3. Yabuuchi N, Kubota K, Dahbi M, Komaba S. Research development on sodium-ion batteries. *Chem Rev*. 2014;114:11636–82.
4. Tang J, Dysart AD, Pol VG. Advancement in sodium-ion rechargeable batteries. *Curr Opin Chem Eng*. 2015;9:34–41.
5. Cao C, Liu W, Tan L, Liao X, Li L. Sodium-ion batteries using ion exchange membranes as electrolytes and separators. *Chem Commun*. 2013;49:11740–2.
6. Wu S, Ge R, Lu M, Xu R, Zhang Z. Graphene-based nano-materials for lithium–sulfur battery and sodium-ion battery. *Nano Energy*. 2015;15:379–405.
7. He H, Li R, Xu Z, Xiao W. An efficient ECC-based mechanism for securing network coding-based P2P content distribution. *Peer-to-Peer Networking Applications*. 2014;7:572–89.
8. Ni'mah YL, Cheng M-Y, Cheng JH, Rick J, Hwang B-J. Solid-state polymer nanocomposite electrolyte of TiO<sub>2</sub>/PEO/NaClO<sub>4</sub> for sodium ion batteries. *J Power Sources*. 2015;278:375–81.
9. Ponrouch A, Monti D, Boschini A, Steen B, Johansson P, Palacin M. Non-aqueous electrolytes for sodium-ion batteries. *J Mater Chem A*. 2015;3:22–42.
10. Kim JG, Son B, Mukherjee S, Schuppert N, Bates A, Kwon O, Choi MJ, Chung HY, Park S. A review of lithium and non-lithium based solid state batteries. *J Power Sources*. 2015;282:299–322.
11. Çakmakçı E, Uğur MH, Güngör A. UV-Cured polypropylene mesh-reinforced composite polymer electrolyte membranes. *e-Polymers* 2015;15:103–10.
12. Ataollahi N, Ahmad A, Lee T, Abdullah A, Rahman MYA. Preparation and characterization of PVDF-MG49-NH<sub>4</sub>CF<sub>3</sub>SO<sub>3</sub> based solid polymer electrolyte. *e-Polymers* 2014;14:115–20.
13. Fenton D, Parker J, Wright P. Complexes of alkali metal ions with poly(ethylene oxide). *Polymer* 1973;14:589.
14. Das S, Ghosh A. Effect of plasticizers on ionic conductivity and dielectric relaxation of PEO-LiClO<sub>4</sub> polymer electrolyte. *Electrochimica Acta*. 2015;171:59–65.
15. Erşahan H, Ekmekyapar A, Sevim F. Flash calcination of a magnesite ore in a free-fall reactor and leaching of magnesite. *Int J Miner Process*. 1994;42:121–36.
16. Patel M, Chandrappa KG, Bhattacharyya AJ. Increasing ionic conductivity of polymer–sodium salt complex by addition of a non-ionic plastic crystal. *Solid State Ionics*. 2010;181:844–8.
17. Mohan V, Raja V, Bhargav PB, Sharma A, Rao VN. Structural, electrical and optical properties of pure and NaLaF<sub>4</sub> doped PEO polymer electrolyte films. *J Polymer Res*. 2007;14:283–90.
18. Mohapatra SR, Thakur AK, Choudhary R. Studies on PEO-based sodium ion conducting composite polymer films. *Ionics* 2008;14:255–62.
19. Berthier C, Gorecki W, Minier M, Armand M, Chabagno J, Rigaud P. Microscopic investigation of ionic conductivity in alkali metal salts-poly(ethylene oxide) adducts. *Solid State Ionics*. 1983;11:91–5.
20. Ferry A, Edman L, Forsyth M, MacFarlane DR, Sun J. NMR and Raman studies of a novel fast-ion-conducting polymer-in-salt electrolyte based on LiCF<sub>3</sub>SO<sub>3</sub> and PAN. *Electrochimica Acta*. 2000;45:1237–42.
21. Boschini A, Johansson P. Characterization of NaX (X: TFSI, FSI)–PEO based solid polymer electrolytes for sodium batteries. *Electrochimica Acta*. 2015;175:124–33.
22. Quartarone E, Mustarelli P. Electrolytes for solid-state lithium rechargeable batteries: recent advances and perspectives. *Chem Soc Rev*. 2011;40:2525–40.
23. Peponi L, Puglia D, Torre L, Valentini L, Kenny JM. Processing of nanostructured polymers and advanced polymeric based nanocomposites. *Mater Sci Eng R Rep*. 2014;85:1–46.
24. Fuentes I, Andrio A, Teixidor F, Viñas C, Compañ V. Enhanced conductivity of sodium versus lithium salts measured by impedance spectroscopy. Sodium cobaltacarboranes as electrolytes of choice. *Phys Chem Chem Phys*. 2017;19:15177–86.
25. Wei D, Meng Q, Jia D. Microstructure of hot-pressed h-BN/Si<sub>3</sub>N<sub>4</sub> ceramic composites with Y<sub>2</sub>O<sub>3</sub>–Al<sub>2</sub>O<sub>3</sub> sintering additive. *Ceram Int*. 2007;33:221–6.
26. Madakbaş S, Çakmakçı E, Kahraman MV. Preparation and thermal properties of polyacrylonitrile/hexagonal boron nitride composites. *Thermochimica Acta*. 2013;552:1–4.
27. Karuppanan KK, Pullithadathil B. A novel biphasic approach for direct fabrication of highly porous, flexible conducting carbon nanofiber mats from polyacrylonitrile (PAN)/NaHCO<sub>3</sub> Nanocomposite. *Microporous Mesoporous Mater*. 2016;224:372–83.
28. Dhakate SR, Gupta A, Chaudhari A, Tawale J, Mathur RB. Morphology and thermal properties of PAN copolymer based electrospun nanofibers. *Synth Met*. 2011;161:411–9.
29. Beevers R. Dependence of the glass transition temperature of polyacrylonitrile on molecular weight. *J Polym Sci A*. 1964;2:5257–65.
30. Tran B, Oladeji IO, Zou J, Chai G, Zhai L. Adhesive poly(PEGMA-co-MMA-co-IBVE) copolymer electrolyte. *Solid State Ionics*. 2013;232:37–43.
31. Kaynak M, Yusuf A, Aydın H, Taşkıran MU, Bozkurt A. Enhanced ionic conductivity in borate ester plasticized Polyacrylonitrile electrolytes for lithium battery application. *Electrochimica Acta*. 2015;164:108–13.
32. Xue TJ, Wilkie CA. Thermal degradation of poly(styrene-g-acrylonitrile). *Polymer Degrad Stab*. 1997;56:109–113.
33. Tutgun MS, Sinirlioglu D, Celik SU, Bozkurt A. Preparation and characterization of hexagonal boron nitride and PAMPS-NMPA-based thin composite films and investigation of their membrane properties. *Ionics*. 2015;21:2871–8.
34. Ekinci KZ, Ünügür Çelik S, Bozkurt A. Enhancing the anhydrous proton conductivity of sulfonated polysulfone/polyvinyl phosphonic acid composite membranes with hexagonal boron nitride. *Int J Polym Mater*. 2015;64:683–9.
35. Tutgun MS, Sinirlioglu D, Celik SU, Bozkurt A. Investigation of nanocomposite membranes based on crosslinked poly(vinyl alcohol)–sulfosuccinic acid ester and hexagonal boron nitride. *J Poly Res*. 2015;22:1–11.
36. Yoon H-K, Chung W-S, Jo N-J. Study on ionic transport mechanism and interactions between salt and polymer chain in PAN based solid polymer electrolytes containing LiCF<sub>3</sub>SO<sub>3</sub>. *Electrochimica Acta*. 2004;50:289–93.